Advances in Nano Research, *Vol. 7 No. 5 (2019) 311-324*
DOI: https://doi.org/10.12989/anr.2019.7.5.311

Nonlocal nonlinear analysis of nano-graphene sheets under compression using semi-Galerkin technique

S.A.M. Ghannadpour* and F. Moradi

New Technologies and Engineering Department, Shahid Beheshti University, G.C, Tehran, Iran

(*Received January 22, 2019, Revised July 19, 2019, Accepted August 4, 2019*)

Abstract. The present study aims to evaluate the nonlinear and post-buckling behaviors of orthotropic graphene sheets exposed to end-shortening strain by implementing a semi-Galerkin technique, as a new approach. The nano-sheets are regarded to be on elastic foundations and different out-of-plane boundary conditions are considered for graphene sheets. In addition, nonlocal elasticity theory is employed to achieve the post-buckling behavior related to the nano-sheets. In the present study, first, out-of-plane deflection function is considered as the only displacement field in the proposed technique, which is hypothesized by an appropriate deflected form. Then, the exact nonlocal stress function is calculated through a complete solution of the von-Karman compatibility equation. In the next step, Galerkin's method is used to solve the unknown parameters considered in the proposed technique. In addition, three different scenarios, which are significantly different with respect to concept, are used to satisfy the natural in-plane boundary conditions and completely attain the stress function. Finally, the post-buckling behavior of thin graphene sheets are evaluated for all three different scenarios, and the impacts of boundary conditions, polymer substrate, and nonlocal parameter are examined in each scenario.

Keywords: nonlocal elasticity; nonlinear behavior; semi-Galerkin technique; nano-graphene sheets; polymer foundation

1. Introduction

Recently, carbon nanostructures have attracted a lot of attention due to their preferred properties. In most of the studies, graphene includes a single layer of carbon atoms, which are joined together by the covalent bond in a two-dimensional honeycomb lattice (Novoselov 2011). Further, it can be implemented in polymer composite materials due to the excellent features of graphene and its high strength value, leading to a reduction of nano-composite weight and an increase in the resistance of polymer composites (Young *et al*. 2012). Graphene sheets can be utilized in different mechanical, optical, electrical, thermal, and chemical fields such as micro-electromechanical systems (MEMS), nano-electromechanical systems (NEMS), sensitive gas sensors, solar cells as well as increasing the resolution of the surface (Jensen *et al*. 2008, Phiri *et al*. 2018).

The way of modelling the nanostructures is considered as an important feature since they involve very small dimensions and limitations in constructing and measuring. Therefore, the experimental modeling is very time-consuming and very expensive (Falvo *et al*. 1998). Along with experimental technique, three general methods are available for modeling these nanostructures such as atomistic modeling (Ball 2001, Li and Chou 2006, Liew *et al*. 2004), continuum mechanics (Wang *et al*. 2006) and hybrid atomistic-continuum mechanics (Li and Chou 2003a, b). Atomistic modeling includes some procedures such as classical molecular dynamics (MD) (Sears and Batra 2004), tight-binding molecular dynamics (TBMD) (Lee *et al*. 2006) and density functional theory (DFT) (Stradi *et al*. 2016) and further, atomistic modeling and hybrid atomistic-continuum mechanics simulations are computationally complex and expensive while the continuum mechanics method is computationally less expensive, compared to other methods, along with its more simple formulation. Thus, this method can be implemented for simulating nanostructures (Duan *et al*. 2010, Wang and Varadan 2006). In small size structures, intermolecular and interatomic cohesive forces can influence the mechanical properties which cannot be disregarded. These effects are demonstrated by length scale parameters in order to formulate continuum mechanics methods. Further, since the classical continuum models disregard the impact of small-scale parameters (Pradhan and Murmu 2009), analyzing the mechanical behavior of graphene sheets based on these models fails to obtain acceptable results. There are some theories which involve the small-scale effects such as couple stress (Akbas 2018, Li and Pan 2015), strain gradient elasticity theory (Bensaid *et al*. 2018, Zibaei *et al*. 2014), micro-morphic (Eringen and Suhubi 1964) and nonlocal elasticity theory (Ebrahimi and Barati 2018, Tavakolian *et al*. 2017).

A large number of researchers have focused on utilizing the Eringen's nonlocal elasticity theory which includes the small-scale effects. According to this theory, the stress at a point relies on the strain of that point, as well as all of the points related to the material (Eringen and Wegner 2003). The nonlocal elasticity theory includes integral and

*Corresponding author, Ph.D.,
E-mail: a_ghannadpour@sbu.ac.ir

ISSN: 2287-237X (Print), 2287-2388 (Online)

differential forms, among which the latter is widely implemented by researchers due to its simplicity. In the present study, the differential form was implemented for analyzing nano-sheets, which may be exposed to different loading conditions due to the variety of their applications. Further, these nano-sheets were considered to be under end-shortening strain. In this situation, buckling, post-buckling, and nonlinear phenomena should be highlighted for these structures. Based on the results of previous studies, the small-scale parameter plays a significant role in the buckling load of the graphene sheets. Therefore, the nonlinear behavior of graphene sheets under compression should be investigated in nano-sheets. Accordingly, the present study aimed to evaluate the nonlinear behavior of graphene sheets under end-shortening strain by utilizing the nonlocal differential elasticity. Thus, a brief overview of the different analyzes of nanoscale structures is required in this regard.

During recent years, the nonlocal elasticity theory has been implemented to analyze the vibration of the beams, plates, as well as shells in micro and nano scales (Chakraverty and Behera 2014, Ghannadpour and Mohammadi 2011, Ehyaei *et al*. 2016, Brischetto *et al*. 2015, Mehar *et al*. 2015). Shen *et al*. (2010) investigated the nonlinear vibration behavior of a single-layer graphene sheet in a thermal environment by focusing on thin plate theory, along with von-Karman geometrical nonlinearity and nonlocal elasticity theory by taking the small effect scale into consideration. In another study, Jomehzadeh *et al*. (2012) examined the free and forced vibration of double-layered graphene sheets embedded in a polymer medium based on the nonlocal elasticity theory. In addition, the van der Waals interactions between polymer medium and graphene sheets were considered as a nonlinear function of deflection of the graphene sheets. Further, Zhang *et al*. (2017) studied the nonlinear vibration behavior of graphene sheets by implementing the classical plate and nonlocal elasticity theories. Furthermore, the size effect was considered and numerical solutions were achieved by using the Kp-Ritz method. Additionally, nonlocal elasticity theory was implemented to analyze the bending of these types of structures on micro and nano scales (Bensaid 2017, Arefi *et al*. 2019, Ghannadpour *et al*. 2013, Taghizadeh *et al*. 2015). In another study, Xu *et al*. (2013) investigated the nonlinear bending of bilayers graphene sheets under transverse loads in thermal environments. Golmakani and Sadraee Far (2016) evaluated the thermo-elastic bending of graphene sheets embedded in the elastic medium by adopting the nonlocal elasticity, and first-order deformation theory, along with von-Karman geometrical model. In order to analyze the buckling behavior of nano-sized structures, a large amount of research have been conducted by using nonlocal elasticity theory (Ghannadpour 2018, Ghannadpour and Mohammadi 2010, Ebrahimi and Barati 2016, Taghizadeh *et al*. 2016, Tounsi *et al*. 2013). For example, Radić and Jeremić (2016) analyzed the thermal buckling of double-layered graphene sheets through adopting the nonlocal elasticity theory and new first-order deformation theory. Further, Anjomshoa *et al*. (2014) analyzed the buckling analysis of multi-layered graphene sheets embedded in a polymer matrix by implementing nonlocal elasticity theory and taking the van der Waals interaction model between graphene sheets and graphene-polymer as a series of linear springs into consideration. During the recent years, few studies were conducted on the post-buckling and nonlinear behaviors of nano-plates by considering the nonlocal elasticity theory. For example, Farajpour *et al*. (2013) evaluated the post-buckling behavior of multi-layered graphene sheets under non-uniform biaxial compression through implementing the nonlocal elasticity theory and von-Karman geometrical model. In another study, Naderi and Saidi (2014) examined the post-buckling behavior of graphene sheets under uniform compression, as well as on a nonlinear polymer substrate by using the nonlocal elasticity theory. In their analysis, the interaction force between graphene sheets and polymer substrate was modeled by a nonlinear function of deflection. In a recent study, Ansari and Gholami (2016) examined the post-buckling behavior of graphene sheets under uniform compression, as well as on a nonlinear polymer substrate by using the nonlocal elasticity theory. In their analysis, the interaction force between graphene sheets and polymer substrate was modeled by a nonlinear function of deflection. More recently, Soleimani *et al*. (2017) emphasized the post-buckling behavior of orthotropic single-layered graphene sheet under in-plane loadings with initial geometric imperfection by applying nonlocal elasticity theory and von-Karman nonlinear model, along with the isogeometric analysis (IGA).

In this research, post-buckling and nonlinear behaviors of orthotropic graphene sheets subjected to end-shortening strain are examined using a new approach called semi-Galerkin technique. The nano-plates are supposed to be on a polymer foundation and the classical plate theory is used to develop the formulation. In the so-called semi-Galerkin technique, similar to the well-known semi-energy approach (Ovesy and Ghannadpour 2011), the out-of-plane deflection is the only displacement field that should be estimated by a deflected form. From the von-Karman type large deflection compatibility equation, the displacement function is related to the stress function in terms of the unknown coefficient in the assumed displacement function. But instead of the theorem of minimum total potential energy in the semi-energy approach, Galerkin method is applied to solve for the unknown coefficients in the proposed technique. Therefore, the introduced method in this paper is called semi-Galerkin technique. The two loaded ends of the graphene sheets are assumed to be simply supported and the others have simple support or clamp conditions. As mentioned earlier, the postulated out-of-plane deflection function is substituted to the von-Karman's compatibility equation and the final equation is exactly solved for the stress function. In order to satisfy the nonlocal natural in-plane boundary conditions, three various scenarios have been assumed and used that are considerably different in terms of concept. Post-buckling behavior of thin graphene sheets are then examined for all three different scenarios and the effects of boundary conditions, polymer foundation and nonlocal parameter have also been studied in each scenario.

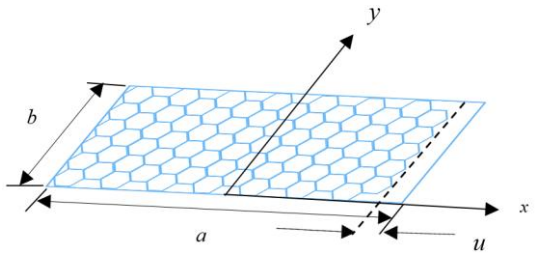

Fig. 1 A typical graphene sheet under end-shortening strain

2. Theoretical development

Consider a typical graphene sheet subjected to end-shortening strain as shown in Fig. 1. The ends under end-shortening are considered to be simply supported and the unloaded edges have either of two following conditions for out-of-plane deflection:

(a) Both unloaded edges are considered to be simply supported.
(b) Both unloaded edges are considered to be clamped

As mentioned before, the purpose of this research is to investigate the post-buckling behavior of nano-plates using nonlocal elasticity theory. According to this theory, the stress at an arbitrary point *x* depends not only on the strain at that point but also on the strain values of all points on the domain of body. The constitutive law based on the nonlocal elasticity theory can be written in the following form (Eringen and Wegner 2003)

$$\sigma_{ij}^{nl}(\underline{x}) = \int_V \alpha\left(\left|\underline{x}-\underline{x}'\right|,\tau\right)\sigma_{ij}^{l}(\underline{x}')dV\,(\underline{x}') \tag{1}$$

where σ_{ij}^{nl}, σ_{ij}^{l} are respectively, nonlocal stress components at the reference point $\underline{x}$ and classical (local) stress components at local point $\underline{x}'$. The parameter α is the nonlocal modulus or kernel function with distance $\left|\underline{x}-\underline{x}'\right|$. This parameter depends on two parameters $\left|\underline{x}-\underline{x}'\right|$ and τ where τ is defined as $e_0\bar{a}/L$. The parameter τ includes the small-scale effects and depends on a material constant (e_0) and characteristic length ratio $\bar{a}/L$, where $\bar{a}$ is an internal characteristic length (e.g., the C-C bond length for graphene sheets, granular distance and lattice parameter) and L is an external characteristic length (e.g., wavelength, crack length and etc.). It is noted that the local stress is written as $\sigma_{ij}^{l} = C_{ijkl}\varepsilon_{kl}$ where C_{ijkl} and ε_{kl} are material moduli and strain components, respectively. In order to work more easily with the constitutive equations in the theory of nonlocal elasticity, the following simple differential form was introduced by Eringen and Wegner (2003) instead of the integral form in Eq. (1)

$$(1-\mu^2\nabla^2)\sigma_{ij}^{nl} = \sigma_{ij}^{l} \tag{2}$$

where $(i,j,k$ and $l=1,2,3)$, ∇^2 is the two dimensional Laplacian mathematical operator and the superscripts "l" and "nl", respectively, denote the local and nonlocal parameters, such as σ_{ij}^{l}, which was previously introduced as local stress. Parameter μ is a nonlocal parameter in nonlocal differential elasticity and is defined as $\mu = e_0\bar{a}$.

Based on the classical plate theory, the displacement fields at a general point can be written in terms of mid-plane components as follows

$$\begin{aligned}\hat{u}(x,y,z) &= u(x,y) - z\frac{\partial w(x,y)}{\partial x}\\ \hat{v}(x,y,z) &= v(x,y) - z\frac{\partial w(x,y)}{\partial y}\\ \hat{w}(x,y,z) &= w(x,y)\end{aligned} \tag{3}$$

where $\hat{u}$, $\hat{v}$ are in-plane and $\hat{w}$ is out of plane components of displacement in x, y and z directions at a general point, respectively, whereas u, v, w are components of displacement at the middle surface of the plate. The strain-displacement relations in the von-Karman form are given as

$$\hat{\varepsilon} = \begin{Bmatrix}\hat{\varepsilon}_x\\ \hat{\varepsilon}_y\\ \hat{\gamma}_{xy}\end{Bmatrix} = \begin{Bmatrix}\dfrac{\partial u}{\partial x}+\dfrac{1}{2}\left(\dfrac{\partial w}{\partial x}\right)^2\\ \dfrac{\partial v}{\partial y}+\dfrac{1}{2}\left(\dfrac{\partial w}{\partial y}\right)^2\\ \dfrac{\partial u}{\partial y}+\dfrac{\partial v}{\partial x}+\left(\dfrac{\partial w}{\partial x}\dfrac{\partial w}{\partial y}\right)\end{Bmatrix} + z\begin{Bmatrix}-\dfrac{\partial^2 w}{\partial x^2}\\ -\dfrac{\partial^2 w}{\partial y^2}\\ -2\dfrac{\partial^2 w}{\partial x\partial y}\end{Bmatrix} = \varepsilon + zk \tag{4}$$

Where $\hat{\varepsilon}_x$, $\hat{\varepsilon}_y$ and $\hat{\gamma}_{xy}$ are components of strains at a general point and ε and k are membrane and curvature strain vectors.

Using the nonlocal constitutive relation in Eq. (2), constitutive relations for a thin orthotropic graphene sheet are given as follows

$$(1-\mu^2\nabla^2)\begin{Bmatrix}\sigma_x^{nl}\\ \sigma_y^{nl}\\ \tau_{xy}^{nl}\end{Bmatrix} = \begin{Bmatrix}\sigma_x^{l}\\ \sigma_y^{l}\\ \tau_{xy}^{l}\end{Bmatrix} = \begin{bmatrix}Q_{11} & Q_{12} & 0\\ Q_{21} & Q_{22} & 0\\ 0 & 0 & Q_{66}\end{bmatrix}\begin{Bmatrix}\hat{\varepsilon}_x\\ \hat{\varepsilon}_y\\ \hat{\gamma}_{xy}\end{Bmatrix} \tag{5}$$

Where the reduced stiffness coefficients Q_{ij} $(i,\ j = 1,2,6)$ can be defined as

$$\begin{aligned}Q_{11} &= \frac{E_1}{1-\nu_{12}\nu_{21}},\quad Q_{22} = \frac{E_2}{1-\nu_{12}\nu_{21}},\\ Q_{12} &= Q_{21} = \frac{\nu_{12}E_2}{1-\nu_{21}\nu_{12}},\quad Q_{66} = G_{12}\end{aligned} \tag{6}$$

It is known that by integrating the components of stress in the thickness direction, the resultant forces and moments can be obtained.

$$\begin{Bmatrix}N_x\\ N_y\\ N_{xy}\end{Bmatrix} = \int_{-h/2}^{h/2}\begin{Bmatrix}\sigma_x\\ \sigma_y\\ \tau_{xy}\end{Bmatrix}dz;\quad \begin{Bmatrix}M_x\\ M_y\\ M_{xy}\end{Bmatrix} = \int_{-h/2}^{h/2}\begin{Bmatrix}\sigma_x\\ \sigma_y\\ \tau_{xy}\end{Bmatrix}zdz \tag{7}$$

By substituting the strains from Eq. (4) into the Eq. (5) and by integrating the results along the thickness, the nonlocal resultant forces and moments are related to the

local ones and membrane and curvature strain vectors in the following form

$$(1-\mu^2\nabla^2)\begin{Bmatrix}N_x^{nl}\\N_y^{nl}\\N_{xy}^{nl}\end{Bmatrix}=\begin{Bmatrix}N_x^{l}\\N_y^{l}\\N_{xy}^{l}\end{Bmatrix}=\begin{bmatrix}A_{11}&A_{12}&0\\A_{12}&A_{22}&0\\0&0&A_{66}\end{bmatrix}\begin{Bmatrix}\varepsilon_x\\\varepsilon_y\\\gamma_{xy}\end{Bmatrix} \quad (8a)$$

$$\begin{aligned}(1-\mu^2\nabla^2)\begin{Bmatrix}M_x^{nl}\\M_y^{nl}\\M_{xy}^{nl}\end{Bmatrix}&=\begin{Bmatrix}M_x^{l}\\M_y^{l}\\M_{xy}^{l}\end{Bmatrix}\\&=\begin{bmatrix}D_{11}&D_{12}&0\\D_{12}&D_{22}&0\\0&0&D_{66}\end{bmatrix}\begin{Bmatrix}k_x\\k_y\\k_{xy}\end{Bmatrix}\end{aligned} \quad (8b)$$

Given that the middle plane strains and curvatures are independent of z, then the above equation can be rewritten in a simpler matrix form as

$$(1-\mu^2\nabla^2)\begin{Bmatrix}N^{nl}\\M^{nl}\end{Bmatrix}=\begin{Bmatrix}N^{l}\\M^{l}\end{Bmatrix}=\begin{bmatrix}A&0\\0&D\end{bmatrix}\begin{Bmatrix}\varepsilon\\k\end{Bmatrix} \quad (9)$$

Where matrices A and D whose coefficients can be obtained by Eq. (10) are extensional and bending stiffness matrices, respectively.

$$A_{ij}=\int_{-\frac{h}{2}}^{\frac{h}{2}}Q_{ij}\,dz,\quad D_{ij}=\int_{-\frac{h}{2}}^{\frac{h}{2}}Q_{ij}z^2\,dz,\quad (i,j=1,2,6) \quad (10)$$

Rearranging the Eq. (9) gives the following matrix form.

$$\begin{Bmatrix}\varepsilon\\M^{l}\end{Bmatrix}=\begin{bmatrix}A^{*}&0\\0&D\end{bmatrix}\begin{Bmatrix}N^{l}\\k\end{Bmatrix} \quad (11)$$

Where $A^{*}=A^{-1}$. The nonlocal equilibrium equations of the graphene sheet based on the classical plate theory can be obtained by the principle of virtual work as follows (Soleimani *et al*. 2017).

$$\frac{\partial N_x^{nl}}{\partial x}+\frac{\partial N_{xy}^{nl}}{\partial y}=0 \quad (12a)$$

$$\frac{\partial N_y^{nl}}{\partial y}+\frac{\partial N_{xy}^{nl}}{\partial x}=0 \quad (12b)$$

$$\begin{aligned}&\frac{\partial^2 M_x^{nl}}{\partial x^2}+\frac{\partial^2 M_y^{nl}}{\partial y^2}+2\frac{\partial^2 M_{xy}^{nl}}{\partial x\partial y}\\&=-\left[N_x^{nl}\frac{\partial^2 w}{\partial x^2}+N_y^{nl}\frac{\partial^2 w}{\partial y^2}+2N_{xy}^{nl}\frac{\partial^2 w}{\partial x\partial y}+P_{vdw-gr}\right]\end{aligned} \quad (12c)$$

The interaction between the polymer foundation and the graphene sheet is simulated by an external transverse load shown as P_{vdw-gr} in the above equation. In this research, this transverse load is considered as a nonlinear function of the deflection like Naderi and Saidi (2014).

$$P_{vdw-gr}=-(K_1w+K_3w^3) \quad (13)$$

A much simpler set of two equations in two unknowns may be achieved by introduction of a nonlocal stress function, φ^{nl}, such that the resultant forces in the nano-plate can be obtained from its derivatives. i.e.

$$N_x^{nl}=\frac{\partial^2\varphi^{nl}}{\partial y^2};\ N_y^{nl}=\frac{\partial^2\varphi^{nl}}{\partial x^2};\ N_{xy}^{nl}=-\frac{\partial^2\varphi^{nl}}{\partial x\partial y} \quad (14)$$

where $\varphi^{nl}=\varphi^{nl}(x,y)$. These expressions are seen to satisfy the first two equilibrium equations (i.e., Eqs. (12a) and (12b)) and the third equilibrium equation can be rewritten as Eq. (15) by combining the Eqs. (4), (8), (11) and (14).

$$\begin{aligned}&D_{11}\frac{\partial^4 w}{\partial x^4}+2(D_{12}+2D_{66})\frac{\partial^4 w}{\partial x^2\partial y^2}+D_{22}\frac{\partial^4 w}{\partial y^4}\\&=(1-\mu^2\nabla^2)\left[\frac{\partial^2\varphi^{nl}}{\partial y^2}\frac{\partial^2 w}{\partial x^2}+\frac{\partial^2\varphi^{nl}}{\partial x^2}\frac{\partial^2 w}{\partial y^2}\right.\\&\left.-2\frac{\partial^2\varphi^{nl}}{\partial x\partial y}\frac{\partial^2 w}{\partial x\partial y}+P_{vdw-gr}\right]\end{aligned} \quad (15)$$

Eqs. (4), (8), (11) and (14) can be combined to give an equation which must be satisfied if the in-plane deformations are to be compatible with the deflection. The nonlocal compatibility equation for graphene sheets can be given in terms of the nonlocal stress function φ^{nl} and w as

$$\begin{aligned}&(1-\mu^2\nabla^2)\left[A_{22}^{*}\frac{\partial^4\varphi^{nl}}{\partial x^4}+(2A_{12}^{*}+A_{66}^{*})\frac{\partial^4\varphi^{nl}}{\partial x^2\partial y^2}\right.\\&\left.+A_{11}^{*}\frac{\partial^4\varphi^{nl}}{\partial y^4}\right]=\left(\frac{\partial^2 w}{\partial x\partial y}\right)^2-\frac{\partial^2 w}{\partial x^2}\frac{\partial^2 w}{\partial y^2}\end{aligned} \quad (16)$$

Eqs. (15) and (16) form two equations in the two variables φ^{nl} and w. They are called the nonlocal equilibrium and compatibility equations, respectively, for large deflections of flat nano-plates. In the next section, the aim is to solve the above equations and obtain the post-buckling response, which requires knowing the in-plane boundary conditions that are referred to below. The out-of-plane boundary conditions of the nano-sheets are also mentioned earlier, and here they are limited to providing their mathematical model.

In-plane boundary conditions on the ends of nano-plates are such that they have zero shear stress conditions and one end is under end-shortening strain as follows.

$$\begin{aligned}&u=0\quad at\quad x=-a/2\\&u=-\varepsilon a\quad at\quad x=a/2\\&N_{xy}^{nl}=0\quad at\quad x=-a/2,a/2\end{aligned} \quad (17)$$

On the unloaded edges, it is assumed in this research that there are only natural boundary conditions such that both shear and normal stresses are assumed to be zero. Thus, they can be written in the following form.

$$N_{xy}^{nl}=N_y^{nl}=0\qquad \text{at}\quad y=0,b \quad (18)$$

As mentioned before, the out-of-plane boundary conditions of the nano-plates is considered to be simply supported on ends, while both the unloaded edges are either simply supported (case (a)) or clamped (case (b)). Therefore

$$\begin{aligned} &w = M_x^{nl} = 0 \quad \text{at } x = -a/2, a/2 \\ &\text{and for both cases (a), (b)} \\ &w = M_y^{nl} = 0 \quad \text{at } y = 0, b \\ &\text{and for case (a)} \\ &w = \partial w/\partial y = 0 \quad \text{at } y = 0, b \\ &\text{and for case } (b) \end{aligned} \tag{19}$$

3. Solution methodology

As previously mentioned, in this paper a new technique called semi-Galerkin technique is introduced and used to investigate the post-buckling and nonlinear behavior of graphene sheets. In this technique, similar to the well-known semi-energy approach (Ovesy and Ghannadpour, 2011), the out-of-plane displacement field is postulated with an appropriate form that can satisfy the nonlocal out-of-plane boundary conditions (cases (a) or (b)). Therefore, from the von-Karman type large deflection compatibility Eq. (16), the displacement function is related to the stress function in terms of the unknown coefficient in the assumed displacement function. In order to solve the stress function in terms of the unknown coefficient in the assumed displacement function and also satisfying the in-plane natural boundary conditions, three different scenarios are considered which are somewhat different in terms of some assumptions. From this point onwards, having the out-of-plane displacement and a stress function, Galerkin method is applied to solve for the unknown coefficient instead of the theorem of minimum total potential energy in the semi-energy approach. In this regard, semi-Galerkin is named for this technique. For the nano-plate shown in Fig. 1, since both ends have simply supported conditions, therefore the out-of-plane deflection form for the post-buckling problem can be considered as follows

$$w(x, y) = \cos(\lambda x) Y(y) \tag{20}$$

where $Y(y)$ is transverse shape function, $\lambda = m\pi/a$ and m is the buckling mode number in the x-direction. The approximation function $\cos(\lambda x)$ satisfies both natural and essential nonlocal boundary conditions along the longitudinal direction (Naderi and Saidi 2014). Due to the different out-of-plane boundary conditions for the unloaded edges, the unknown function $Y(y)$ is first used to represent the out-of-plane deflection form along the transverse direction and therefore all the equations are solved in terms of this unknown function. Finally, after solving and developing the formulation, in the last step, the estimation function will be replaced with respect to the boundary conditions in this direction.

As it was mentioned earlier, the assumed out-of-plane deflection form (i.e., Eq. (20)) should be substituted in the nonlocal compatibility equation for graphene sheets (i.e., Eq. (16)) to solve the nonlocal stress function. But finding a relationship between local and nonlocal stress function can help to further the solution. Using Eqs. (2), (8) and (14), this equation is obtained as

$$(1 - \mu^2 \nabla^2)\varphi^{nl} = \varphi^{l} \tag{21}$$

In the above equation, φ^l and φ^{nl} are local and nonlocal stress functions, respectively.

Therefore, having the above relation and substituting the Eq. (20) into the nonlocal compatibility Eq. (16), the following equation is achieved

$$\begin{aligned} &A_{22}^* \frac{\partial^4 \varphi^l}{\partial x^4} + (A_{66}^* + 2A_{12}^*) \frac{\partial^4 \varphi^l}{\partial x^2 \partial y^2} + A_{11}^* \frac{\partial^4 \varphi^l}{\partial y^4} \\ &= \frac{1}{2}\lambda^2 \{[Y'^2 + YY''] + [YY'' - Y'^2]\cos(2\lambda x)\} \end{aligned} \tag{22}$$

Where $Y' = dY/dy$ and $Y'' = d^2Y/dy^2$. It can be understood from the above equation that one can first calculate the local stress function and then calculate the nonlocal stress function using Eq. (21). Then the main problem is solving based on the local elasticity. To solve the local stress function, it is also clear from the above equation that the local stress function φ^l can be written as a sum of two distinct functions as follows (Ovesy and Ghannadpour 2011).

$$\varphi^l = \varphi_1^l + \varphi_2^l \cos(2\lambda x) \tag{23}$$

Where $\varphi_1^l = \varphi_1^l(y)$ and $\varphi_2^l = \varphi_2^l(y)$. Subsequently, the derivative of functions φ_1^l and φ_2^l with respect to y that are just a function of y, are represented by the prime sign. By substituting the Eq. (23) into Eq. (22) and equating the coefficients on both sides of the equation, the following relationships are achieved.

$$A_{11}^* \varphi_1^{l\,''''} = \frac{1}{2}\lambda^2 [Y'^2 + YY''] \tag{24a}$$

$$\begin{aligned} &A_{11}^* \varphi_2^{l\,''''} - 4(A_{66}^* + 2A_{12}^*)\lambda^2 \varphi_2^{l\,''} + 16A_{22}^* \lambda^4 \varphi_2^l \\ &= \frac{1}{2}\lambda^2 [YY'' - Y'^2] \end{aligned} \tag{24b}$$

Given the above equations, now the two functions $\varphi_1^l(y)$ and $\varphi_2^l(y)$ need to be solved.

3.1 Solution of function $\varphi_1^l(y)$

By twice integrating the Eq. (24a), the following equation is obtained in which the second derivative of φ_1^l constitutes a stress system in the *x*-direction. It is noteworthy that only the second derivative of φ_1^l is required in the calculations and does not need to evaluate the function itself.

$$\varphi_1^{l\,''} = \frac{1}{4A_{11}^*}\lambda^2 Y^2 + C_1 y + C_2 \tag{25}$$

where the constants C_1 and C_2 are used to satisfy the in-plane boundary conditions (17) at the loaded ends. From Eq. (4), the following relationship can be written.

$$u|_{-a/2}^{a/2} = \int_{-a/2}^{a/2} \left\{ \varepsilon_x - \frac{1}{2}\left(\frac{\partial w}{\partial x}\right)^2 \right\} dx \tag{26}$$

Both Eqs. (11) and (14) are combined so that the amount of end-shortening can be expressed in terms of the deflection and local stress function.

$$u|_{-a/2}^{a/2} = \int_{-a/2}^{a/2} \left\{ A_{11}^* \frac{\partial^2 \varphi^l}{\partial y^2} + A_{12}^* \frac{\partial^2 \varphi^l}{\partial x^2} - \frac{1}{2}\left(\frac{\partial w}{\partial x}\right)^2 \right\} dx \tag{27}$$

By substituting the deflection function from Eq. (20) and local stress function from Eq. (23) in the above expression and performing the integration, the amount of end-shortening of the nano-sheet can be computed as

$$u|_{-a/2}^{a/2} = aA_{11}^* {\varphi_1^l}'' - \frac{a}{4}\lambda^2 Y^2 \tag{28}$$

Substituting the second derivative of φ_1^l from Eq. (25) into Eq. (28) yields

$$u|_{x=a/2} - u|_{x=-a/2} = aA_{11}^*(C_1 y + C_2) \tag{29}$$

Since the end of the sheet at $x = a/2$ is uniformly shortened (i.e., $u = -\varepsilon a$ from Eq. (17)), so it does not change with respect to y, and therefore the constant C_1 is zero and the constant C_2 is also computed as

$$C_2 = -\frac{\varepsilon}{A_{11}^*} \tag{30}$$

The value of C_2 is the stress required to compress the unbuckled plate. Substituting C_1 and C_2 in Eq. (25), the second derivative of φ_1^l is now obtained as

$${\varphi_1^l}'' = \frac{1}{4A_{11}^*}\lambda^2 Y^2 - \frac{\varepsilon}{A_{11}^*} \tag{31}$$

3.2 Solution of function $\varphi_2^l(y)$

As is known, Eq. (24b) is a fourth order non-homogeneous linear differential equation. Solving it involves a general or homogeneous solution φ_{2h}^l and a particular solution φ_{2p}^l. In order to obtain a homogeneous solution, the following fourth order homogeneous differential equation is considered.

$$\begin{aligned} &A_{11}^* {\varphi_{2h}^l}'''' - 4(A_{66}^* + 2A_{12}^*)\lambda^2 {\varphi_{2h}^l}'' \\ &+16A_{22}^*\lambda^4 \varphi_{2h}^l = 0 \end{aligned} \tag{32}$$

where the "*h*" and "*p*" indexes refer to the homogeneous and particular solutions of φ_2^l. The homogeneous solution to the above equation depends on the Δ sign, which Δ is defined as follows

$$\Delta = (A_{66}^* + 2A_{12}^*)^2 - 4A_{11}^* A_{22}^* \tag{33}$$

For different signs of Δ the homogeneous solution to Eq. (32) can be presented as follows.

(1) If $\Delta > 0$, the general solution φ_{2h}^l can be written in the following form

$$\begin{aligned} \varphi_{2h}^l &= C_1^\varphi \cosh(2\lambda_1 \lambda y) \\ &+C_2^\varphi \sinh(2\lambda_1 \lambda y) + C_3^\varphi \cosh(2\lambda_2 \lambda y) \\ &+C_4^\varphi \sinh(2\lambda_2 \lambda y) \end{aligned} \tag{34}$$

Where $\lambda_1 = \sqrt{\dfrac{2A_{12}^* + A_{66}^* + \sqrt{\Delta}}{2A_{11}^*}}$ and $\lambda_2 = \sqrt{\dfrac{2A_{12}^* + A_{66}^* - \sqrt{\Delta}}{2A_{11}^*}}$.

(2) If $\Delta = 0$, the homogeneous solution can be represented as

$$\begin{aligned} &\varphi_{2h}^l = \\ &C_1^\varphi \cosh(2\bar{\lambda}\lambda y) + C_2^\varphi \sinh(2\bar{\lambda}\lambda y) + C_3^\varphi \, y\cosh(2\bar{\lambda}\lambda y) \\ &+C_4^\varphi y \sinh(2\bar{\lambda}\lambda y) \end{aligned} \tag{35}$$

Where $\bar{\lambda} = \sqrt[4]{\dfrac{A_{22}^*}{A_{11}^*}}$

(3) If $\Delta < 0$, the φ_{2h}^l can be written as

$$\begin{aligned} &\varphi_{2h}^l = \\ &\left(C_1^\varphi \cos(2\lambda_2 \lambda y) + C_2^\varphi \sin(2\lambda_2 \lambda y)\right)\cosh(2\lambda_1 \lambda y) \\ &+\left(C_3^\varphi \cos(2\lambda_2 \lambda y) + C_4^\varphi \sin(2\lambda_2 \lambda y)\right)\sinh(2\lambda_1 \lambda y) \end{aligned} \tag{36}$$

Where $\lambda_1 = \dfrac{1}{2}\sqrt{2\sqrt{\dfrac{A_{22}^*}{A_{11}^*}} + \dfrac{2A_{12}^* + A_{66}^*}{2A_{11}^*}}$ and $\lambda_2 = \dfrac{1}{2}\sqrt{2\sqrt{\dfrac{A_{22}^*}{A_{11}^*}} - \dfrac{2A_{12}^* + A_{66}^*}{2A_{11}^*}}$.

In the above solutions, the constants $C_i^\varphi (i = 1,..,4)$ can be calculated depending on the in-plane boundary conditions of the unloaded edges. Finding these constants and satisfying the natural boundary conditions has led to the suggestion of three different scenarios which will be further dealt with in this section.

So far the general solution has been calculated, but the particular solution, whose function is also considered, is related to the right-hand side function of the inhomogeneous Eq. (24b). By substituting the deflection form along the y-direction, $Y(y)$, into the Eq. (24b) and using the undetermined coefficients method, the particular solution can be computed that will be presented for each boundary conditions (cases (a) or (b)) in the next section. By finding the homogeneous and the particular solution, complete solution to φ_2^l is determined as

$$\varphi_2^l = \varphi_{2h}^l + \varphi_{2p}^l \tag{37}$$

Up to now, the second derivate of φ_1^l and local stress function φ_2^l in which there are four constants $C_i^{\varphi}(i = 1,..,4)$, have been fully calculated. At this point, to fulfill the natural in-plane boundary conditions, several scenarios can be designed to solve the constants which are discussed in the next section.

3.3 Calculate C_i^{φ} constants

As previously stated, in order to solve the nonlocal stress function in terms of the unknown coefficient in the assumed deflection function and also fulfilment of the natural in-plane boundary conditions, three different scenarios are designed which are somewhat different in terms of some assumptions.

It should be emphasized that many scientists in their research have satisfied only the local form of natural boundary conditions to analyze their nonlocal problems such as works carried out by Jomehzadeh and Saidi (2011a, b), Jomehzadeh *et al*. (2012), Shen *et al*. (2010) and some other researchers have corrected their formulation and results and have been able to fulfill the nonlocal natural boundary conditions (Naderi and Saidi 2014, Wang *et al*. 2007). With these descriptions, in this research, it is also desirable to study the effects of these conditions on the post-buckling behavior of nano-sheets by satisfying the local form of natural boundary conditions or nonlocal forms. The following is a description of the designed scenarios.

3.3.1 Scenario 1

In this scenario, it is assumed that the local form of the compatibility equation is used to obtain the results by setting $\mu = 0$ in Eq. (16). Therefore, all previous equations are still established. The four constants $C_i^{\varphi}(i = 1,..,4)$ in the local stress function $\varphi^l(x,y)$ should then be computed by satisfying the local form of natural in-plane boundary conditions on the unloaded edges, thus the stress function $\varphi^l(x,y)$ is now fully specified. The concept of this scenario, in accordance with the claim of Naderi and Saidi (2014) is similar to the assumptions considered in Jomehzadeh *et al*. (2012), Jomehzadeh and Saidi (2011a, b), Shen *et al*. (2010), which have investigated nonlinear free vibration of nano-plates.

With the descriptions outlined in this scenario, the local stress function, which was calculated instead of the nonlocal stress function, is substituted in the equilibrium equation (i.e., Eq. (15)) for the next steps of the solution.

3.3.2 Scenario 2

As in the previous scenario, the local stress function is calculated in the same way. Similarly, as in Scenario 1, the local form of natural boundary conditions applies to the calculation of constants $C_i^{\varphi}(i = 1,..,4)$ in the local stress function φ^l. As is clear from Eq. (21), two nonlocal and local forms of stress function are related to each other. It can be easily shown that the nonlocal stress function can be written in terms of the corresponding local stress function in the following form.

$$\varphi^{nl}(x,y) = \varphi^l(x,y) + \mu^2\nabla^2\varphi^l(x,y) + \mu^4\nabla^4\varphi^l(x,y) + \mu^6\nabla^6\varphi^l(x,y) + \cdots \quad (38)$$

Therefore, after calculating the local stress function φ^l described in the above, the nonlocal form of stress function φ^{nl} is obtained through Eq. (38). It should be noted that the solution of the nonlocal stress function in Eq. (38) is identical to the particular solution of Eq. (21), and therefore, one can use the particular solution of Eq. (21) instead of using the above equation. To find the particular solution, one can proceed as follows.

Similar to the local stress function, by substituting the deflection function from Eq. (20) into the compatibility equation, it can be seen that the nonlocal stress function can also be written in the form below.

$$\varphi^{nl}(x,y) = \varphi_1^{nl}(y) + \varphi_2^{nl}(y)\cos(2\lambda x) \quad (39)$$

By substituting Eqs. (23) and (39) into Eq. (21) and rearranging, the following two equations can be written

$$[4\lambda^2\mu^2 + 1]\varphi_2^{nl} - \mu^2\varphi_2^{nl''} = \varphi_2^l \quad (40a)$$

$$\varphi_1^{nl} - \mu^2\varphi_1^{nl''} = \varphi_1^l \quad (40b)$$

Since the local stress function, φ_1^l, has not been solved itself and its second derivative has been calculated, therefore, its second derivative, $\varphi_1^{l''}$, can be substituted into Eq. (40b) and the second derivative of the nonlocal stress function, $\varphi_1^{nl''}$, is obtained, which is required in the next steps. Both the particular solution of the above equations are used to form the nonlocal stress function φ^{nl}.

Therefore, it is emphasized that in this scenario, the constants $C_i^{\varphi}(i = 1,..,4)$ are calculated by satisfying the local form of natural boundary conditions, but the nonlocal form of stress function, according to Eq. (21), is substituted in the equilibrium equation.

3.3.3 Scenario 3

The difference between this scenario with Scenario 2 is to satisfy the nonlocal natural boundary conditions rather than its local form. In this scenario, as in the previous scenario, the nonlocal stress function is calculated in terms of the local stress function, but this time, with all four unknown constants $C_i^{\varphi}(i = 1,..,4)$. That is, the unknown constants are not already obtained by satisfying the local form of natural boundary conditions. Finally, they can be computed by satisfying the nonlocal natural boundary conditions. Therefore, having the nonlocal stress function, the equilibrium equation is ready for use in the next section. It is noteworthy that the detailed process in this scenario is more logical and the results are supposed to be compared with the outcomes of other scenarios in which there are drawbacks in satisfying the boundary conditions.

3.4 Calculate C_i^{φ} constants

In this section, having a stress function by each of the scenarios introduced in the previous section, as well as by

assuming the deflection function for any given boundary conditions, the equilibrium Eq. (15) can be rewritten in terms of the unknown deflection coefficient and a residual function R is determined. To find this unknown coefficient for any prescribed end-shortening strain, the well-known Galerkin method is applied as follows.

$$\int_{-a/2}^{a/2}\int_{0}^{b} R\phi \, dx \, dy = 0 \tag{41}$$

Where ϕ is a weight function that should be appropriately selected. After solving the nonlinear algebraic equation obtained from the above integral and calculating the unknown deflection coefficient, the average longitudinal force N_{av} can be determined by integrating the nonlocal resultant force N_x^{nl} over the plate domain.

$$N_{av} = \frac{1}{ab}\int_{-a/2}^{a/2}\int_{0}^{b} N_x^{nl} \, dx \, dy \tag{42}$$

Therefore, all standard post-buckling curves, including load-deflection and load-end shortening curves, can be represented for any desired example.

4. Results and discussion

The formulations developed in this research have been implemented in Maple for analyzing the post-buckling and nonlinear behaviors of graphene sheets on a polymer foundation under end-shortening strain. As mentioned in the formulation section, the nano-sheets that are being investigated here have two different out-of-plane boundary conditions. The ends under end-shortening were considered to be simply supported and the unloaded edges have either simply supported condition (cases (a)) or clamped condition (cases (b)). Therefore, the out-of-plane deflection function in the transverse direction $Y(y)$ can be estimated with respect to the boundary conditions of the cases (a) and (b).

For case (a)

$$Y(y) = \bar{W}\sin\left(\frac{n\pi}{b}y\right) \tag{43}$$

and for the clamped condition (case(b)), it can be approximated as follows

$$Y(y) = \bar{W}\sin\left(\frac{n\pi}{b}y\right) \tag{44}$$

Where n is the buckling mode number in the y-direction. Therefore, the buckling mode in the presentation of results is shown as (m,n). In order to obtain the numerical results, graphene sheets with two different dimensions as well as two different materials are used in this study. These materials are zigzag and armchair graphene. The material properties for armchair graphene sheet are (Naderi and Saidi 2014)

$E_1 = 1949$ GPa, $E_2 = 1962$ GPa, $\upsilon_{12} = 0.201$,
$G_{12} = 846$ GPa, $\mu = 0.27$ nm

and its thickness is assumed to be 0.156 nm. Also, the dimensions of armchair graphene sheets are considered to be $a = 4.888$ nm and $b = 4.855$ nm. The material properties of zigzag graphene sheet are also taken from Naderi and Saidi (2014) as

$E_1 = 1987$ GPa, $E_2 = 1974$ GPa, $\upsilon_{12} = 0.205$,
$G_{12} = 857$ GPa, $\mu = 0.22$ nm

The thickness and dimensions of zigzag graphene sheets are considered as 0.154 nm, $a = 1.987$ nm and $b = 1.974$ nm. By selecting the materials described above, the Δ sign is negated according to Eq. (33), and therefore, the form of Eq. (36) is used as a homogenous solution to Eq. (36) for the local stress function φ_{2h}^{l}. It is also assumed that the armchair and zigzag graphene sheets being on a polymer substrate made of polyethylene (Jomehzadeh *et al.* 2012). Linear and nonlinear interaction coefficients k_1 and k_3 are assumed to be, respectively, 28.4941 GPa/nm and 12825.3287 GPa/nm.

Figs. 2 and 3 show the variation of average longitudinal force N_{av} versus the non-dimensional maximum deflection w/h of the sheets based on both local and nonlocal theories for armchair and zigzag graphene sheets, respectively. The results presented in both figures have been obtained for graphene sheets with all edges simply supported (i.e., boundary conditions case (a)) being on a polyethylene substrate. It was seen that armchair graphene sheet buckles

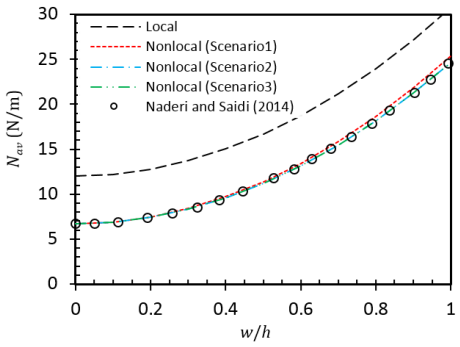

Fig. 2 Longitudinal force-maximum deflection behavior for armchair graphene sheet with BCs case (a) on a polymer substrate

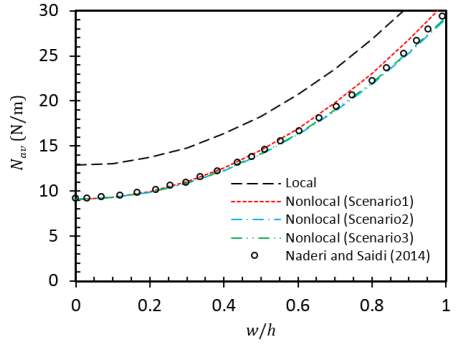

Fig. 3 Longitudinal force-maximum deflection behavior for zigzag graphene sheet with BCs case (a) on a polymer substrate

in mode (6,1) while the buckling mode for the zigzag sheet is (2,1). Therefore, the post-buckling results for these two nano-sheets have been obtained according to their buckling modes. To validate and compare the nonlocal results, the post-buckling results obtained by using the nonlocal elasticity theory and carried out by Naderi and Saidi (2014) are also presented in these figures. As can be seen from these figures, and as expected, there is a significant difference between the critical buckling loads as well as post-buckling behaviors based on both local and nonlocal elasticity theories. In order to investigate the effects of satisfying the local form of natural in-plane boundary conditions or nonlocal forms, as outlined in the previous section, the results acquired in this study have been reported for all three detailed scenarios. Therefore, such results can also be found in Figs. 2 and 3 for armchair and zigzag graphene sheets.

It can also be observed from these figures that there is not much difference between the results of different scenarios when the nano-sheets are on a polyethylene foundation, except for Scenario 1, in which only the local stress function was used and the nonlocal stress function was not calculated at all. Also, it is seen that the results of the second and third scenarios are very close to those reported by Naderi and Saidi (2014). Load variations in terms of end-shortening strain, which indicate the nonlinear behavior of sheets under compression, are also shown in Figs. 4 and 5 for armchair and zigzag graphene sheets in accordance with Figs. 2 and 3, respectively. Similar to Figs. 2 and 3, the results have been presented for both local and nonlocal theories and for all three scenarios and the sheets are on polymer substrate too. In addition to the descriptions for Figs. 2 and 3, it is also observed that the critical strain of the nonlocal graphs is lower than the local critical strain. Therefore, the nonlocal theory of elasticity estimates lower values for critical buckling load and its corresponding strain and it also considers the structure to be more prone to buckling. It is also seen that the results of Naderi and Saidi (2014) shown in Figs. 2 and 3, do not exist on this figure because such results have not been obtained by Naderi and Saidi (2014). On the other hand, the formulation presented in that research is not able to calculate the amount of end-shortening strain.In order to study different out-of-plane boundary conditions and also to observe possible differences between the scenarios in these boundary conditions, variations of load versus non-dimensional maximum deflection and versus end-shortening strain for zigzag graphene sheet with two clamped unloaded edges (i.e., boundary conditions case (b)) are depicted in Figs. 6 and 7, respectively. However, the buckling mode, in this boundary conditions type, is (3,1) and it's still assumed that the nano-sheet is on the polyethylene foundation.

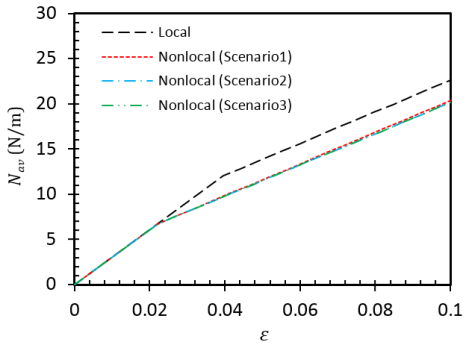

Fig. 4 Longitudinal force-end shortening behavior for armchair graphene sheet with BCs case (a) on a polymer substrate

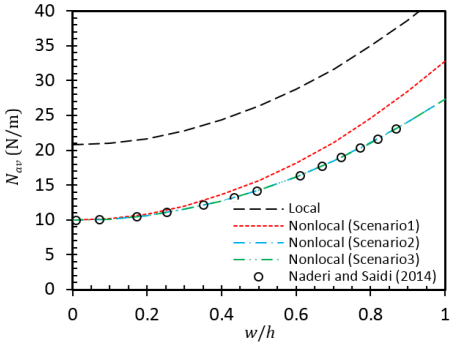

Fig. 6 Longitudinal force-maximum deflection behavior for zigzag graphene sheet with BCs case (b) on polymer foundation

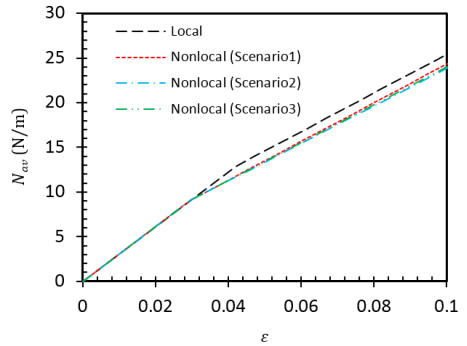

Fig. 5 Longitudinal force-end shortening behavior for zigzag graphene sheet with BCs case (a) on a polymer substrate

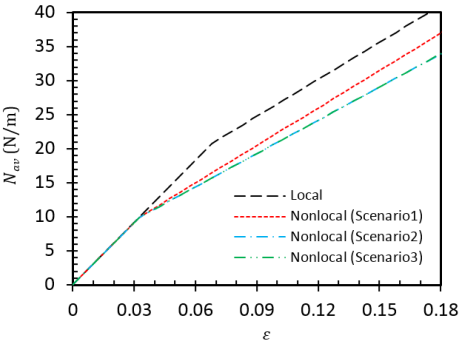

Fig. 7 Longitudinal force-end shortening behavior for zigzag graphene sheet with BCs case (b) on polymer substrate

As seen in all above figures, there is no significant difference between the scenarios particularly between scenarios 2 and 3. The reason for the lack of a serious difference between the results of different scenarios is the placement of the nano-sheets on the polyethylene foundation. The presence of such a foundation makes the sheets stiffer and reduces the amount of deflections, and therefore the lateral in-plane movement of the unloaded edges of the nano-sheets are also reduced. Reducing this movement (which corresponds to the transverse in-plane stresses), makes no significant difference in how the local and nonlocal forms of natural boundary conditions are satisfied. The polymer substrate has also led to no significant difference in the results of critical buckling loads of the nano-sheets with different boundary conditions. Therefore, nano-sheets without polymer substrate will be analyzed further to see these effects. To this end, post-buckling behaviors of the armchair and zigzag graphene sheets without polyethylene foundation are shown in Figs. 8 to 13. Both local and nonlocal results are incorporated in these figures and the nonlocal results have been obtained for all three scenarios. Also, different boundary conditions, cases (a) and (b), are considered to obtain the results presented here. To compare the achieved nonlocal results in this study, the formulation developed by Naderi and Saidi (2014) was fully implemented and the results are also incorporated into the figures.

As can be seen in these figures, there are noteworthy differences between the three scenarios related to the nonlocal theory. In other words, it can be stated that when the polymer foundation is not considered in the post-buckling analysis, the nonlocality effects have a more significant impact on the outcomes, and therefore imprecise satisfaction of the natural boundary conditions results in inaccurate results.

Therefore, it can be concluded that with the presence of foundation, the satisfaction of local or nonlocal natural in-plane boundary conditions (i.e., each of the scenarios 2 or 3) does not significantly affect the accuracy of the outcomes, whereas, in the absence of the substrate, satisfaction of the local natural boundary conditions will lead to completely wrong results. It is also seen in these figures that the results extracted from the assumptions of Scenario 3, which are the most correct way to satisfy the natural boundary conditions, are much closer to the results obtained by the formulation developed by Naderi and Saidi (2014).

As observed in the results, the results of Scenario 3 showed the best fit with those obtained by Naderi and Saidi (2014). This excellent conformance, which appears on the graphical figures, apparently reflects the similarity of the results of both formulations. But it should be noted that the results are not numerically the same and are slightly different. It seems that there may be two factors that make

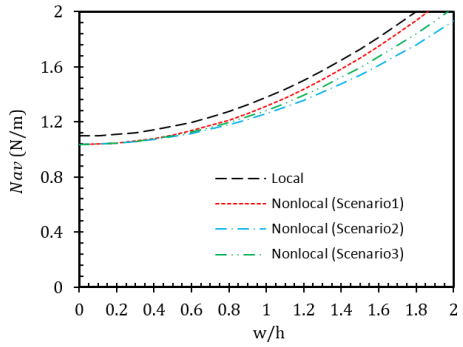

Fig. 8 Longitudinal force-maximum deflection behavior for armchair graphene sheet with BCs case (a) without polymer substrate

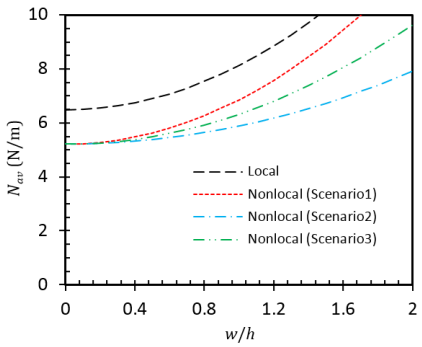

Fig. 10 Longitudinal force-maximum deflection behavior for zigzag graphene sheet with BCs case (a) without polymer substrate

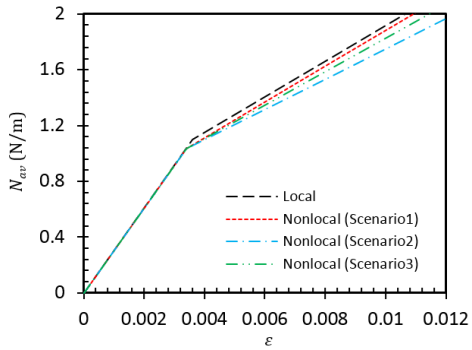

Fig. 9 Longitudinal force-end shortening behavior for armchair graphene sheet with BCs case (a) without polymer substrate

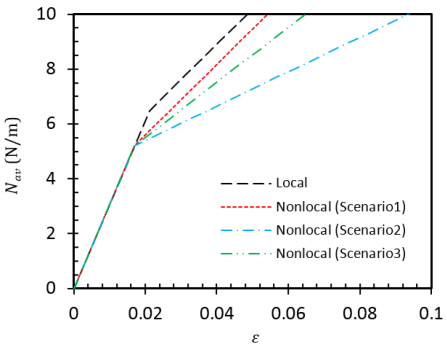

Fig. 11 Longitudinal force-end shortening behavior for zigzag graphene sheet with BCs case (a) without polymer substrate

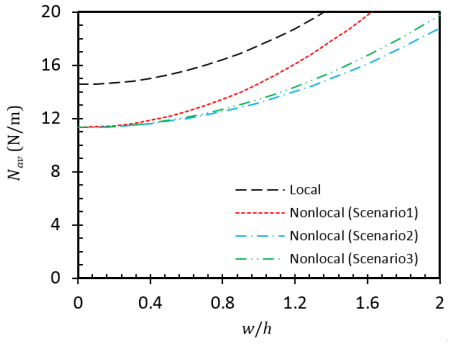

Fig. 12 Longitudinal force-maximum deflection behavior for zigzag graphene sheet with BCs case (b) without polymer substrate

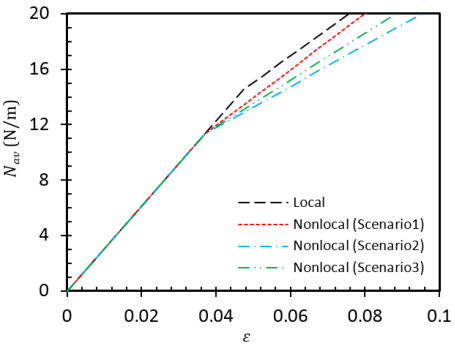

Fig. 13 Longitudinal force-end shortening behavior for zigzag graphene sheet with BCs case (b) without polymer substrate

this difference: one is how to apply the loading, which in this study is uniformly end-shortening, but in (Naderi and Saidi 2014) is uniformly compressive load, and the other is that the general solution for the nonlocal compatibility equation and for solving the stress function in (Naderi and Saidi 2014) is just a simple solution satisfying the in-plane boundary conditions and not the exact solution of the compatibility equation. However, in the present study, the compatibility equation is exactly solved and in addition to its particular solution, its homogenous solution is also completely obtained and then the nonlocal boundary conditions are satisfied. It seems that with the technique presented in (Naderi and Saidi 2014), one cannot obtain an appropriate response for other boundary conditions. To illustrate this numerical difference, the presented formulation in (Naderi and Saidi 2014) was implemented exactly and its results are compared with the results from Scenario 3 in this study, as shown in the following table. The results presented in Table 1 are average longitudinal forces N_{av} for zigzag graphene sheets.

As it is seen, the results correspond to $w/h = 0$ (i.e., the buckling loads) are exactly the same, and there is no difference between the two formulations. It should be noted that both of the factors mentioned above, which led to the differences in the results, are not related to the buckling load, and therefore the results are the same as expected. But as soon as the sheets buckle and enter to the post-buckling region (i.e., the out-of-plane displacements other than zero), the uniform distribution of the buckling load is no longer present, and also the exact solution to the compatibility equation is important, which is, of course, related to the actual distribution of the in-plane stresses of the sheets. So the differences start from here. However, these differences do not appear in the graphs. It is also observed that the difference between the results is more pronounced for plates without polymer substrate and it also increases as the nonlocal parameter increases.

In the last step, the effects of the nonlocal parameter on the longitudinal force-maximum deflection and longitudinal force-end shortening strain behaviors of simply supported

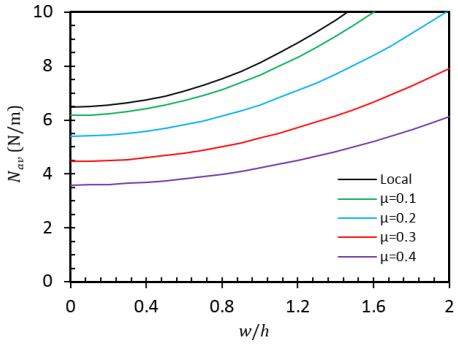

Fig. 14 Effect of the nonlocal parameter on longitudinal force-maximum deflection behavior for zigzag graphene sheet with BCs case (a)

Table 1 Comparison of the loads N_{av} from Scenario 3 with those from the formulation presented in (Naderi and Saidi 2014)

Case	$\frac{w}{h}$	On nonlinear polymer substrate				Without polymer substrate			
		$\mu = 0.1$		$\mu = 0.2$		$\mu = 0.1$		$\mu = 0.2$	
		Naderi and Saidi (2014)	Scenario3	Naderi and Saidi (2014)	Scenario3	Naderi and Saidi (2014)	Scenario3	Naderi and Saidi (2014)	Scenario3
(a)	0	11.7417	11.7417	9.5149	9.5149	6.1697	6.1697	5.3943	5.3943
	0.5	17.1005	17.0863	14.6195	14.6272	6.6899	6.5440	5.8025	5.6879
	1	33.1767	33.1202	29.9336	29.9642	8.2505	7.6669	7.0272	6.5686
(b)	0	16.7927	16.8264	10.8702	10.8702	13.7428	13.7428	11.7810	11.7810
	0.5	21.9772	22.0216	15.3605	15.3604	14.5235	14.4155	12.4398	12.3336
	1	37.5308	37.6074	28.8315	28.8312	16.8654	16.4336	14.4161	13.9914

zigzag graphene sheets without polymer substrate can be seen in Figs. 14 and 15, respectively. Similar results are presented in Figs. 16 and 17 for zigzag graphene sheets with two clamped unloaded edges (case (b)). The results have been obtained by using Scenario 3 in which the satisfaction of boundary conditions has been implemented correctly and are compared with those obtained by local elasticity theory. It can be seen from these figures that as the nonlocal parameter increases, the buckling load reduces noticeably and the post-buckling stiffness reduction also increases.

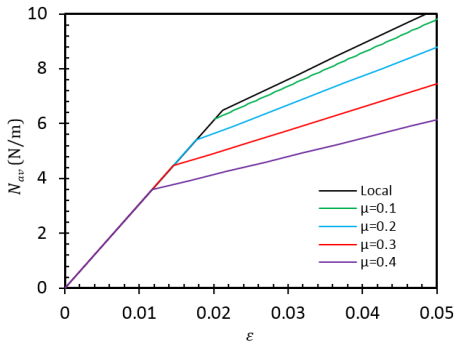

Fig. 15 Effect of the nonlocal parameter on the variation of longitudinal force with end shortening for zigzag graphene sheet with BCs case (a)

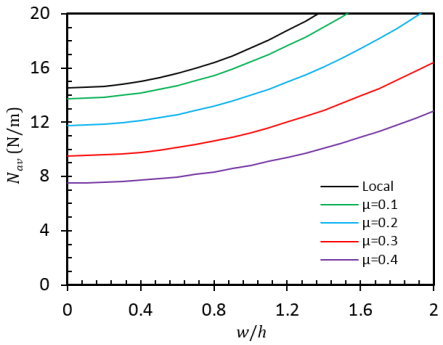

Fig. 16 Effect of the nonlocal parameter on longitudinal force-maximum deflection behavior for zigzag graphene sheet with BCs case (b)

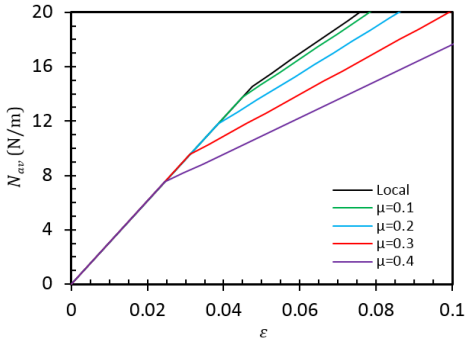

Fig. 17 Effect of the nonlocal parameter on the variation of longitudinal force with end shortening for zigzag graphene sheet with BCs case (b)

5. Conclusions

This paper has outlined a new approach called semi-Galerkin technique for studying the post-buckling and nonlinear behaviors of orthotropic zigzag and armchair graphene sheets with or without polymer substrate. The nano-sheets were analyzed with the assumption that they were subjected to the end-shortening strain and the theory used for post-buckling analysis was nonlocal elasticity theory. The exact nonlocal stress function was calculated by solving the nonlocal compatibility equation and the nonlocal von-Karman equilibrium equation was solved using the Galerkin method. In order to obtain a complete stress function and calculate the constants, and also to investigate the effects of satisfying the local form or nonlocal form of natural in-plane boundary conditions, three different scenarios were designed and used to obtain the results. These scenarios were different in terms of satisfying the local form or nonlocal form of the natural in-plane boundary conditions. It was found that although Scenario 3 was the correct scenario, there is not much difference between the results of second and third scenarios when the nano-sheets are on a polymer foundation. The presence of polymer foundation makes the sheets stiffer and reduces the amount of deflections, and therefore the lateral in-plane movement of the unloaded edges of the nano-sheets are also reduced and it makes no significant difference in how the natural boundary conditions are satisfied. But instead, it was seen that when the polymer foundation is not considered in the post-buckling analysis, the nonlocality effects had a more significant impact on the outcomes, and therefore imprecise satisfaction of the natural boundary conditions results in inaccurate results.

References

Akbas, S.D. (2018), "Forced vibration analysis of cracked functionally graded microbeams", *Adv. Nano Res., Int. J.*, **6**(1), 39-55. https://doi.org/10.12989/anr.2018.6.1.039

Anjomshoa, A., Shahidi, A.R., Hassani, B. and Jomehzadeh, E. (2014), "Finite element buckling analysis of multi-layered graphene sheets on elastic substrate based on nonlocal elasticity theory", *Appl. Math. Model*, **38**, 5934-5955. https://doi.org/10.1016/j.apm.2014.03.036

Ansari, R. and Gholami, R. (2016), "Size-dependent nonlinear vibrations of first-order shear deformable magneto-electro-thermo elastic nanoplates based on the nonlocal elasticity theory", *Int. J. Appl. Mech.*, **8**, 1650053. https://doi.org/10.1142/S1758825116500538

Arefi, M., Mohammad-Rezaei Bidgoli, E., Dimitri, R., Bacciocchi, M. and Tornabene, F. (2019), "Nonlocal bending analysis of curved nanobeams reinforced by graphene nanoplatelets", *Compos. Part B Eng.*, **166**, 1-12. https://doi.org/10.1016/j.compositesb.2018.11.092

Ball, P. (2001), "Roll up for the revolution", *Nature*, **414**, 142-144. https://doi.org/10.1038/35102721

Bensaid, I. (2017), "A refined nonlocal hyperbolic shear deformation beam model for bending and dynamic analysis of nanoscale beams", *Adv. Nano Res., Int. J.*, **5**(2), 113-126. https://doi.org/10.12989/anr.2017.5.2.113

Bensaid, I., Bekhadda, A. and Kerboua, B. (2018), "Dynamic analysis of higher order shear-deformable nanobeams resting on

elastic foundation based on nonlocal strain gradient theory", *Advances Nano Res., Int. J.*, **6**(3), 279-298. https://doi.org/10.12989/anr.2018.6.3.279

Brischetto, S., Tornabene, F., Fantuzzi, N. and Bacciocchi, M. (2015), "Refined 2D and exact 3D shell models for the free vibration analysis of single-and double-walled carbon nanotubes", *Technologies*, **3**(4), 259-284. https://doi.org/10.3390/technologies3040259

Chakraverty, S. and Behera, L. (2014), "Free vibration of rectangular nanoplates using Rayleigh-Ritz method", *Phys. E Low-Dimens. Syst. Nanostruct.*, **56**, 357-363. https://doi.org/10.1016/j.physe.2013.08.014

Duan, W.H., Wang, Q., Wang, Q. and Liew, K.M. (2010), "Modeling the instability of carbon nanotubes: from continuum mechanics to molecular dynamics", *J. Nanotechnol. Eng. Med.*, **1**, 11001. https://doi.org/10.1115/1.3212820

Ebrahimi, F. and Barati, M.R. (2016), "Analytical solution for nonlocal buckling characteristics of higher-order inhomogeneous nanosize beams embedded in elastic medium", *Adv. Nano Res., Int. J.*, **4**(3), 229-249. https://doi.org/10.12989/anr.2016.4.3.229

Ebrahimi, F. and Barati, M.R. (2018), 'Stability analysis of functionally graded heterogeneous piezoelectric nanobeams based on nonlocal elasticity theory", *Adv. Nano Res., Int. J.*, **6**(2), 93-112. https://doi.org/10.12989/anr.2018.6.2.093

Ehyaei, J., Ebrahimi, F. and Salari, E. (2016), "Nonlocal vibration analysis of FG nano beams with different boundary conditions", *Adv. Nano Res., Int. J.*, **4**(2), 85-111. https://doi.org/10.12989/anr.2016.4.2.085

Eringen, A.C. and Suhubi, E.S. (1964), "Nonlinear theory of simple micro-elastic solids—I", *Int. J. Eng. Sci*., **2**, 189-203. https://doi.org/10.1016/0020-7225(64)90004-7

Eringen, A. and Wegner, J. (2003), *Nonlocal Continuum Field Theories*, *Applied Mechanics Reviews*, Springer, New York, NY, USA.

Falvo, M.R., Clary, G., Helser, A., Paulson, S., Taylor, R.M., Chi, V., Brooks, F.P., Washburn, S. and Superfine, R. (1998), "Nanomanipulation experiments exploring frictional and mechanical properties of carbon nanotubes", *Microsc. Microanal*, **4**, 504-512. https://doi.org/10.1017/S1431927698980485

Farajpour, A., Solghar, A.A. and Shahidi, A. (2013), "Postbuckling analysis of multi-layered graphene sheets under non-uniform biaxial compression", *Phys. E Low-Dimens. Syst. Nanostruct.*, **47**, 197-206. https://doi.org/10.1016/j.physe.2012.10.028

Ghannadpour, S.A.M. (2018), "Ritz method application to bending, buckling and vibration analyses of Timoshenko beams via nonlocal elasticity", *J. Appl. Comput. Mech*., **4**, 16-26. https://doi.org/10.22055/JACM.2017.21915.1120

Ghannadpour, S.A.M. and Mohammadi, B. (2010), "Buckling Analysis of Micro- and Nano-Rods/Tubes Based on Nonlocal Timoshenko Beam Theory Using Chebyshev Polynomials", *Adv. Mater. Res*., **123**, 619-622. https://doi.org/10.4028/www.scientific.net/AMR.123-125.619

Ghannadpour, S.A.M. and Mohammadi, B. (2011), "Vibration of nonlocal Euler beams using Chebyshev polynomials", *Key Eng. Mater*., **471**, 1016-1021. https://doi.org/10.4028/www.scientific.net/KEM.471-472.1016

Ghannadpour, S.A.M., Mohammadi, B. and Fazilati, J. (2013), "Bending, buckling and vibration problems of nonlocal Euler beams using Ritz method", *Compos. Struct*., **96**, 584-589. https://doi.org/10.1016/j.compstruct.2012.08.024

Golmakani, M.E. and Sadraee Far, M.N. (2016), "Nonlinear thermo-elastic bending behavior of graphene sheets embedded in an elastic medium based on nonlocal elasticity theory", *Comput. Math. Appl*., **72**, 785-805. https://doi.org/10.1016/j.camwa.2016.06.022

Jensen, K., Kim, K. and Zettl, A. (2008), "An atomic-resolution nanomechanical mass sensor", *Nat. Nanotechnol*., **3**(9), 533. https://doi.org/10.1038/nnano.2008.200

Jomehzadeh, E. and Saidi, A.R. (2011a), "Decoupling the nonlocal elasticity equations for three dimensional vibration analysis of nano-plates", *Compos. Struct*., **93**, 1015-1020. https://doi.org/10.1016/j.compstruct.2010.06.017

Jomehzadeh, E. and Saidi, A.R. (2011b), "A study on large amplitude vibration of multilayered graphene sheets", *Comput. Mater. Sci.*, **50**, 1043-1051. https://doi.org/10.1016/j.commatsci.2010.10.045

Jomehzadeh, E., Saidi, A.R. and Pugno, N.M. (2012), "Large amplitude vibration of a bilayer graphene embedded in a nonlinear polymer matrix", *Phys. E Low-Dimensional Syst. Nanostruct.*, **44**, 1973-1982. https://doi.org/10.1016/j.physe.2012.05.015

Lee, G. Do, Wang, C.Z., Yoon, E., Hwang, N.M. and Ho, K.M. (2006), "Vacancy defects and the formation of local haeckelite structures in graphene from tight-binding molecular dynamics", *Phys. Rev. B - Condens. Matter Mater. Phys*., **74**(24), 245411. https://doi.org/10.1103/PhysRevB.74.245411

Li, C. and Chou, T.W. (2003a), "A structural mechanics approach for the analysis of carbon nanotubes", *Int. J. Solids Struct*., **40**(10), 2487-2499. https://doi.org/10.1016/S0020-7683(03)00056-8

Li, C. and Chou, T.W. (2003b), "Single-walled carbon nanotubes as ultrahigh frequency nanomechanical resonators", *Phys. Rev. B - Condens. Matter Mater. Phys*., **68**(7), 073405. https://doi.org/10.1103/PhysRevB.68.073405

Li, C. and Chou, T.W. (2006), "Elastic wave velocities in single-walled carbon nanotubes", *Phys. Rev. B - Condens. Matter Mater. Phys*., **73**(24), 245407. https://doi.org/10.1103/PhysRevB.73.245407

Li, Y.S. and Pan, E. (2015), "Static bending and free vibration of a functionally graded piezoelectric microplate based on the modified couple-stress theory", *Int. J. Eng. Sci*., **97**, 40-59. https://doi.org/10.1016/j.ijengsci.2015.08.009

Liew, K.M., Wong, C.H., He, X.Q., Tan, M.J. and Meguid, S.A. (2004), "Nanomechanics of single and multiwalled carbon nanotubes", *Phys. Rev. B - Condens. Matter Mater. Phys*., **69**(11), 115429. https://doi.org/10.1103/PhysRevB.69.115429

Mehar, K., Panda, S.K., Dehengia, A. and Kar, V.R. (2015), "Vibration analysis of functionally graded carbon nanotube reinforced composite plate in thermal environment", *J. Sandw. Struct. Mater.*, **18**(2), 151-173. https://doi.org/10.1177/1099636215613324

Naderi, A. and Saidi, A.R. (2014), "Nonlocal postbuckling analysis of graphene sheets in a nonlinear polymer medium", *Int. J. Eng. Sci*., **81**, 49-65. https://doi.org/10.1016/j.ijengsci.2014.04.004

Novoselov, K.S. (2011), "Nobel Lecture: Graphene: Materials in the Flatland", *Rev. Mod. Phys*., **83**, 837-849. https://doi.org/10.1103/RevModPhys.83.837

Ovesy, H.R. and Ghannadpour, S.A.M. (2011), "An exact finite strip for the initial postbuckling analysis of channel section struts", *Comput. Struct*., **89**, 1785-1796. https://doi.org/10.1016/j.compstruc.2010.10.009

Phiri, J., Johansson, L.S., Gane, P. and Maloney, T. (2018), "A comparative study of mechanical, thermal and electrical properties of graphene-, graphene oxide- and reduced graphene oxide-doped microfibrillated cellulose nanocomposites", *Compos. Part B Eng*., **147**, 104-113. https://doi.org/10.1016/j.compositesb.2018.04.018

Pradhan, S.C. and Murmu, T. (2009), "Small scale effect on the buckling of single-layered graphene sheets under biaxial compression via nonlocal continuum mechanics", *Comput. Mater. Sci*., **47**, 268-274.

https://doi.org/10.1016/j.commatsci.2009.08.001
Radić, N. and Jeremić, D. (2016), "Thermal buckling of double-layered graphene sheets embedded in an elastic medium with various boundary conditions using a nonlocal new first-order shear deformation theory", *Compos. Part B Eng*., **97**, 201-215. https://doi.org/10.1016/j.compositesb.2016.04.075
Sears, A. and Batra, R.C. (2004), "Macroscopic properties of carbon nanotubes from molecular-mechanics simulations", *Phys. Rev. B - Condens. Matter Mater. Phys.*, **69**(23), 235406. https://doi.org/10.1103/PhysRevB.69.235406
Shen, L., Shen, H.-S. and Zhang, C.-L. (2010), "Nonlocal plate model for nonlinear vibration of single layer graphene sheets in thermal environments", *Comput. Mater. Sci*., **48**, 680-685. https://doi.org/10.1016/j.commatsci.2010.03.006
Soleimani, A., Naei, M.H. and Mosavi Mashadi, M. (2017), "Nonlocal postbuckling analysis of graphene sheets with initial imperfection based on first order shear deformation theory", *Results Phys*., **7**, 1299-1307. https://doi.org/10.1016/j.rinp.2017.03.003
Stradi, D., Martinez, U., Blom, A., Brandbyge, M. and Stokbro, K. (2016), "General atomistic approach for modeling metal-semiconductor interfaces using density functional theory and nonequilibrium Green's function", *Phys. Rev. B*, **93**, 155302. https://doi.org/10.1103/PhysRevB.93.155302
Taghizadeh, M., Ovesy, H.R. and Ghannadpour, S.A.M. (2015), "Nonlocal integral elasticity analysis of beam bending by using finite element method", *Struct. Eng. Mech*., *Int. J*., **54**, 755-769. https://doi.org/10.12989/sem.2015.54.4.755
Taghizadeh, M., Ovesy, H.R. and Ghannadpour, S.A.M. (2016), "Beam buckling analysis by nonlocal integral elasticity finite element method", *Int. J. Struct. Stab. Dyn*., **16**, 1550015. https://doi.org/10.1142/S0219455415500157
Tavakolian, F., Farrokhabadi, A. and Mirzaei, M. (2017), "Pull-in instability of double clamped microbeams under dispersion forces in the presence of thermal and residual stress effects using nonlocal elasticity theory", *Microsyst. Technol*., **23**, 839-848. https://doi.org/10.1007/s00542-015-2785-z
Tounsi, A., Benguediab, S., Adda, B., Semmah, A. and Zidour, M. (2013). "Nonlocal effects on thermal buckling properties of double-walled carbon nanotubes", *Adv. Nano Res., Int. J.*, **1**(1), 1-11. https://doi.org/10.12989/anr.2013.1.1.001
Wang, Q. and Varadan, V.K. (2006), "Wave characteristics of carbon nanotubes", *Int. J. Solids Struct*., **43**, 254-265. https://doi.org/10.1016/j.ijsolstr.2005.02.047
Wang, C.M., Tan, V.B.C. and Zhang, Y.Y. (2006), "Timoshenko beam model for vibration analysis of multi-walled carbon nanotubes", *J. Sound Vib*., **294**, 1060-1072. https://doi.org/10.1016/j.jsv.2006.01.005
Wang, C.M., Zhang, Y.Y. and He, X.Q. (2007), "Vibration of nonlocal Timoshenko beams", *Nanotechnology*, **18**(10), 105401. https://doi.org/10.1088/0957-4484/18/10/105401
Xu, Y.M., Shen, H.S. and Zhang, C.L. (2013), "Nonlocal plate model for nonlinear bending of bilayer graphene sheets subjected to transverse loads in thermal environments", *Compos. Struct*., **98**, 294-302. https://doi.org/10.1016/j.compstruct.2012.10.041
Young, R.J., Kinloch, I.A., Gong, L. and Novoselov, K.S. (2012), "The mechanics of graphene nanocomposites: A review", *Compos. Sci. Technol*., **72**, 1459-1476. https://doi.org/10.1016/j.compscitech.2012.05.005
Zhang, L.W., Zhang, Y. and Liew, K.M. (2017), "Modeling of nonlinear vibration of graphene sheets using a meshfree method based on nonlocal elasticity theory", *Appl. Math. Model*., **49**, 691-704. https://doi.org/10.1016/j.apm.2017.02.053
Zibaei, I., Rahnama, H., Taheri-Behrooz, F. and Shokrieh, M.M. (2014), "First strain gradient elasticity solution for nanotube-reinforced matrix problem", *Compos. Struct*., **112**, 273-282. https://doi.org/10.1016/j.compstruct.2014.02.023

CC